REVISTA INTERDISCIPLINAR DE PESQUISA EM ENGENHARIA

CILAMCE 2016
XXXVII IBERIAN LATIN AMERICAN CONGRESS ON COMPUTATIONAL METHODS IN ENGINEERING
BRASÍLIA - DF - BRAZIL

# HYDRODYNAMIC BEHAVIOR ANALYSIS OF A SCHOOL BOAT USING CFD

**Daniel Freitas Coelho**

daniel.coelho@itec.ufpa.br / dancoelhoptr@gmail.com

FEM / UFPA

Rua Augusto Corrêa, 1, 66075-110, Pará, Belém, Brazil

**André Luiz Amarante Mesquita**

andream@ufpa.br / andreamarantemesquita@hotmail.com

TECNOLAGO / NDAE / UFPA

Vila Permanente, Rodovia BR 422, 68464-000, Pará, Tucuruí, Brazil

***Abstract.*** *High amplitude wave wake due to water flow on a school boat hull can prejudice directly residents of riverside communities by inducing erosions, damage to fixed or floating structures and also, damage to smaller boats, fishermen and swimmers. Therefore, designers introduced wave deflector surfaces in a new fleet of school boats to reduce the amplitude of the boat wave wake. In this study, the applicability of these surfaces were evaluated using computational tools. Initially, a multiphasic computational model of a Wigley hull was created in order to validate the numerical model. The validation model had good accordance compared to experimental results, with errors below 7% for resistance coefficient. Later, the school boat model was compared with images from the real operating school boat, where similarities between the two were observed. Models with different operation points were created. Finally, the comparison with, and without the wave deflector surfaces made it possible to notice the wave amplitude reduction. The wave deflector showed a efficiency improvement for velocities from 17.5 up to 20 km/h, above the usual operation speed of 15 km/h, which makes your use unfavorable. The methodology adopted was consistent and it can be used for a large range of investigations of this type.*

***Keywords:*** *School boat, Wigley hull, CFD, Free surface, VOF method*

# 1 INTRODUCTION

In the Amazon region, even nowadays students from riverside communities continue with access difficulties to school environments. This routine of going to school can be even harder during rainy seasons due to regional climate changes. In addition to that, during dry seasons can be impossible to sail because the low water levels, and due to that the river courses are covered by mud.

According to FNDE (2010) 300,000 children in Brazil need waterway transport to get to classrooms. Only in Brazilian northern region, and at least 208 cities throughout Brazil needs to be provided with decent transportation. In this sense, FNDE developed a project to design a new fleet of school boats, which could avoid school dropout by ensuring comfort and security to the students.

Together with the implementation of the new boat fleet, new problems may appear in the local communities due to the new fleet of boats, which could be harmful to the environment. Some examples are pollution of the rivers and atmosphere, arise of noise and high amplitude wave wakes. The last one not only annoys anglers and swimmers, but most importantly impairs residents of riverside communities by inducing erosions, damaging fixed or floating structures (Kofoed-Hanson, Mikkelsen, 1997; Stumbo, 1999).

The wave wake behavior can be a complex phenomenon near the boat surroundings, which relies on the hull shape, velocity and many other parameters. On the other hand, it becomes simpler at great distances from the boat and can be defined by the Kelvin wake pattern (Souza and Aguiar, 2001).

The wave is generated mainly by pressure gradients near the waterline. Therefore, if pressure is high on a side of the hull near the waterline, it will generate a local wave crest and a transversal wave behind that. According to Raven (2010), high pressure regions can occur near stagnation points, in the bow area, at concave streamwise curvatures and at large streamwise slopes.

There are several ways to simulate the wave wake. Pressure can be calculated without the free surface VOF (Volume of Fluid) approach with great accuracy but only for Froude numbers below 0.2 (Raven, 2010). Including free surface on the calculations, the wave amplitude can be obtained and the physics can be well represented. Other authors have done the validation of commercial softwares using the free surface approach (Gao, Yang and Xie, 2015; Pranzitelli, Nicola and Miranda, 2011; Ahmed, 2011; Banks, Phillips and Turnock, 2010).

This paper will highlight the hydrodynamic evaluation of a school boat hull using ANSYS Fluent and adopting the VOF (Hirt and Nichols, 1981) open channel approach. Two cases will be compared: with and without wave deflector surfaces. The application of these wave deflectors in theory can reduce the wave amplitudes along the river. The fuel consumption will be evaluated as well, since it is directly attached to the hull resistance or drag.

In order to investigate the applicability of a computational fluid dynamics (CFD) code, the Wigley hull case was used on the hull resistance and the wave pattern prediction. It is a classical case for multiphasic flows since it has open experimental results and the hull surface is equation driven.

After the validation, the hydrodynamic of the school boat is evaluated for different operation conditions (velocities between 15 and 25 km/h). Images from the real operating boat are compared with the numerical results in order to review the similarities of the numerical model with the real physics.

## 2 SCHOOL BOAT

The school boat used for this study has its geometry described by Figs. 1 and 2 where 9 transversal profiles are used to define the geometry. The transversal profiles positions are obtained in Fig. 1 and their curves in Fig. 2. The wave deflector surfaces are highlighted, and general dimensions of the school boat are presented at Table 1.

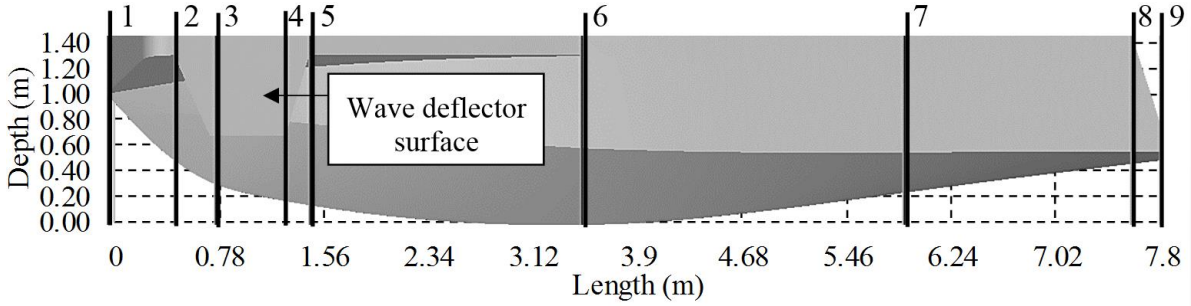


**Figure 1. Longitudinal profile of the school boat hull**

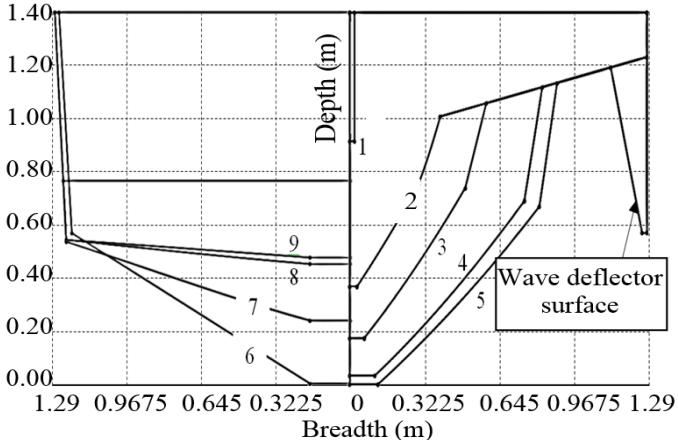


**Figure 2. Transversal profiles of the school boat hull**

**Table 1. General dimensions of the school boat**

| Constitutive relation | Value |
|---|---|
| Length | 7.80 m |
| Breadth | 2.55 m |
| Draft | 0.67 m |
| Usual speed | 15 km/h |
| Capacity | 20 passengers + 1 crew |

## 3 PHYSICAL MODEL

The physical model consists of water flow and air through the hull surface. The control volume is delimited by non-physical walls, which have to be positioned on a distance large enough so that they do not influence the flow inside the control volume and do not create an artificial acceleration field by the blockage effect.

Since air resistance on the hull is negligible, the deck extension through the control volume does not result in significant errors. In addition, since the hull is symmetric, it is assumed that the flow is symmetric as well; therefore, it is a standard practice to use only half of the domain.

The physical model can be described as a multiphasic flow with immiscible fluids (water and air), where these fluids were considered to be incompressible and the flow to be turbulent. All variables and properties are shared by the phases and represent volume-averaged values (VOF assumption). Water flow through the hull is considered not oblique and the environment generates no waves near the hull. Hull translation and rotation effects are neglected as well.

# 4 MATHEMATICAL MODEL

The governing equations for the CFD calculations are integrated over each control volume, such that relevant quantities (mass, momentum, energy etc.) are conserved in a discrete sense for each control volume. In Reynolds averaging, the solution variables in the instantaneous (exact) Navier-Stokes equations are decomposed into the mean (time-averaged) and fluctuating components. By substituting expressions of this form for the flow variables into the instantaneous continuity and momentum equations and taking their time average yields the ensemble-averaged momentum equations (ANSYS Inc., 2006). Considering incompressible Newtonian fluid, the Reynolds-averaged Navier-Stokes (RANS) equations can be written in Cartesian tensor form, respectively as:

$$\frac{\partial \rho}{\partial t} + \frac{\partial}{\partial x_j}\left(\rho \overline{u_j}\right) = 0 \tag{1}$$

$$\frac{\partial}{\partial t}\left(\rho \overline{u_i}\right) + \frac{\partial}{\partial x_j}\left(\rho \overline{u_i u_j}\right) = \frac{\partial}{\partial x_j}\left\{ -\overline{p}\delta_{ij} + \mu\left(\frac{\partial \overline{u_i}}{\partial x_j} + \frac{\partial \overline{u_j}}{\partial x_i}\right) - \rho \overline{u_i' u_j'} \right\} + \rho g_i . \tag{2}$$

Where $\overline{u_i}$ (i = 1,2,3) and $\overline{u_j}$ (j = 1,2,3) are the components of averaged velocity, $\overline{p}$ is the mean pressure, $\delta_{ij}$ is the Kronecker delta, $\rho$ is the fluid density, $\mu$ is the fluid dynamic viscosity and the term $-\rho \overline{u_i' u_j'}$ is the advection of momentum or Reynolds stress ($\tau_{ij}$), which results in the spread of momentum by turbulence.

Since there are no explicit governing differential equations for the additional unknowns due to the Reynolds stress term, the problem is indeterminate. One needs to close the problem to obtain a solution. Therefore, the turbulence modeling tries to represent the Reynolds stresses in terms of the time-averaged velocity components and close the problem.

Multiple turbulence models were created to calculate these parameters. The turbulence model chosen was SST k-ω because it retains the robust and accurate formulation of the k-ω model in the near wall region and takes advantage of the freestream independence of the k-ε model in the outer part of the boundary-layer (Menter, 1994). Additional information about this turbulence model can be found in Menter (1994).

# 5 COMPUTATIONAL MODEL

## 5.1 Simulation methodology

It is important to notice that in any simulation process using CFD applications, it is almost impossible to obtain satisfactory results on the first try and so, it is usual to return a few steps in order to obtain a better solution with good convergence and similarity with experimental results. Satisfactory results can be defined as errors below 10% (sometimes even greater error values are accepted), results consistent with the physics of the problem, convergence, mass balance etc.

## 5.2 Configuration set-up

Let L be the hull length, the bottom surface was at 1L below the waterline, while inflow and outflow surfaces were placed respectively at 1L and 2L from the model. The side surface

is located at 2L from the symmetry plane. Since the region occupied by air has to be modelled, the top surface is placed at 1L above the waterline to ensure that the air has room enough to flow through the waves and does not artificially accelerate due to a blockage effect.

For the mesh, the use of tetrahedral grids can lead to the diffusion of the volume fraction. Thus, the use of higher order solution schemes and smaller time steps are needed to maintain a sharp interface. Hexahedral grids, on the other hand, can provide better results with less processing time. For the validation case 761,940 elements were generated. For the school boat 2,380,327 elements were generated without the wave deflector and 2,375,887 elements with it. A higher number of elements were applied at the design waterline. Pranzitelli, Nicola and Miranda (2011) adopted a value of $y^+$ below 100 and had great agreement with experimental results. This value was adopted in this investigation as well.

A problem often encountered in presence of waves is their reflection on nonphysical boundaries of the flow field, which causes oscillations on the coefficient of resistance and wave elevation. Therefore, the introduction of numerical diffusion is useful to avoid reflection at the boundaries of the domain. This can be done using a strong growth rate of cell dimension from the model to the external boundaries (Pranzitelli, Nicola and Miranda, 2011).

For the Fluent set-up, multiphasic flow was modelled using Open Channel Flow VOF implicit with Compressive scheme, p-v coupling used was Coupled with Volume Fractions; momentum and turbulence parameters were discretized using the QUICK scheme.

## 5.3 Boundary conditions

The boundary conditions assigned to the inlet and outlet are pressure-inlet and pressure-outlet respectively, same as Pranzitelli, Nicola and Miranda (2011). It may be odd to select pressure for both inlet and outlet but when selecting open channel flow, flow velocity and free surface height are requested on pressure-inlet boundary condition, and so the pressure is calculated based on hydrostatic pressure formula and the volume fraction is obtained based on the free surface height.

The velocity on the inlet ($U_\infty$) for the Wigley hull validation case is calculated using Eq. (3) where $F_N$ is the Froude number, g is the gravity and L is the hull length. The resistance tests and wave pattern measurement are done based on $F_N$ from 0.25 to 0.4. For the school boat, 5 different velocities were defined (15 km/h, 17.5 km/h, 20 km/h, 22.5 km/h and 25 km/h).

$$U_\infty = F_N \sqrt{gL} \tag{3}$$

In many CFD applications, geometry and boundary conditions are symmetric on a plane. In those cases, it is usual to adopt a symmetry boundary condition. This helps reducing the computational effort by reducing the number of mesh elements and also improves the solution convergence. At the hull and deck, no-slip wall boundary conditions are imposed. Finally, free slip wall boundary condition was assigned to the non-physical walls.

# 6 VALIDATION CASE

In order to validate the CFD application for the school boat on resistance and wave pattern prediction, experimental data for a Wigley hull case (Kajitani et al., 1983) was used. The hull shape can be determined for x, y and z axes by the Eq. (4) where L, B and D is hull length, breadth and draft, respectively. Values adopted for L, B and D were 4 m, 0.4 m and 0.25 m.

$$y = \frac{2B}{L}\left[1-\left(\frac{2x}{L}\right)^2\right]\left[1-\left(\frac{z}{D}\right)^2\right] \tag{4}$$

The results obtained for the validation of the numerical model through a comparison to the Wigley experimental data are showed at Figs. 3 and 4. Figure 3-a exhibits the hull total resistance coefficient. The resistance coefficient can be calculated by Eq. (5) where $R_t$ is the resistance force and S is the wetted surface. Figure 3-b exhibits the numerical-experimental relative error ($\%\Delta C_t = 100|C_t^{exp} - C_t^{num}|/C_t^{exp}$). Figure 4 shows the dimensionless wave elevation ($\xi$) curve results for different Froude numbers. It can be obtained from Eq. (6) where $\zeta$ is the real wave elevation. It is possible to observe that the numerical model showed a good agreement to the experimental data.

$$C_t = \frac{R_t}{0.5\rho U_\infty{}^2 S} \qquad S = 0.661L(2D+B) \tag{5}$$

$$\xi = 2g\zeta / U_\infty{}^2 \tag{6}$$

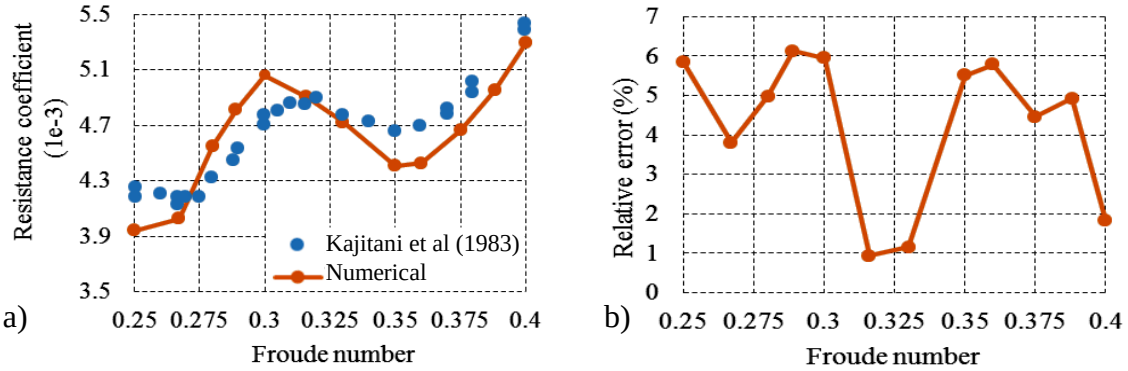


**Figure 3. Resistance coefficients (a) and relative error (b) comparing numerical and experimental results varying Froude number**

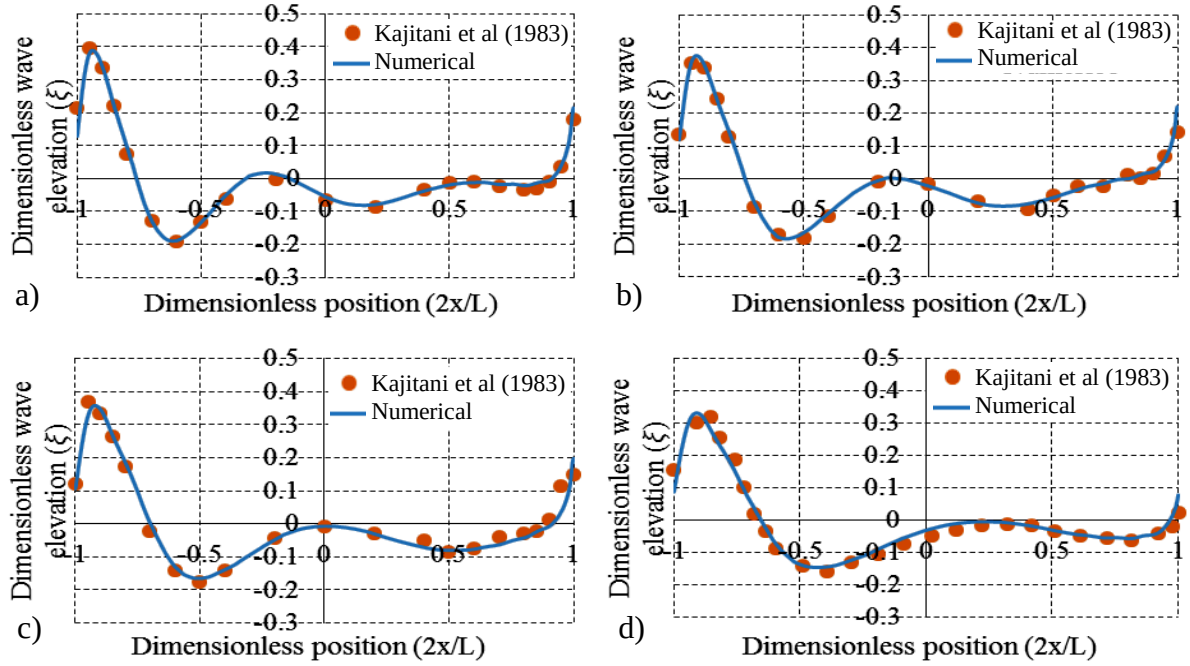


**Figure 4. Dimensionless wave elevation for Froude numbers 0.250 (a), 0.267 (b), 0.289 (c) and 0.316 (d).**

# 7 CASE STUDY: SCHOOL BOAT

## 7.1 Flow analysis

Since there were no experimental results concerning this kind of investigation for the school boat, a qualitative analysis was adopted to verify the numerical results. This analysis consists on the comparison of images of the real school boat in operation with the numerical results. It is important to notice that this is not the best methodology to validate the numerical results, since the real boat is not in a controlled environment. Nevertheless, this can be considered a good starting point to obtain reference values of wave elevation.

In this sense, Fig. 5 and 6 exhibits the comparison between the real school boat in operation with a velocity of 15 km/h and the numerical results considering velocities of 15, 17.5, and 20 km/h, where the latter represents the design speed. Figures 5-b and 6-b represents the free surface (water-air interface) and its coloring indicates the values of free surface elevation starting from the waterline. It is clearly seen in the real school boat picture (see Fig. 6-a) that there is a wave pattern through the external surface of the wave deflector due to the oblique flow reaching the hull. The numerical model could not predict this pattern since oblique flow was not considered.

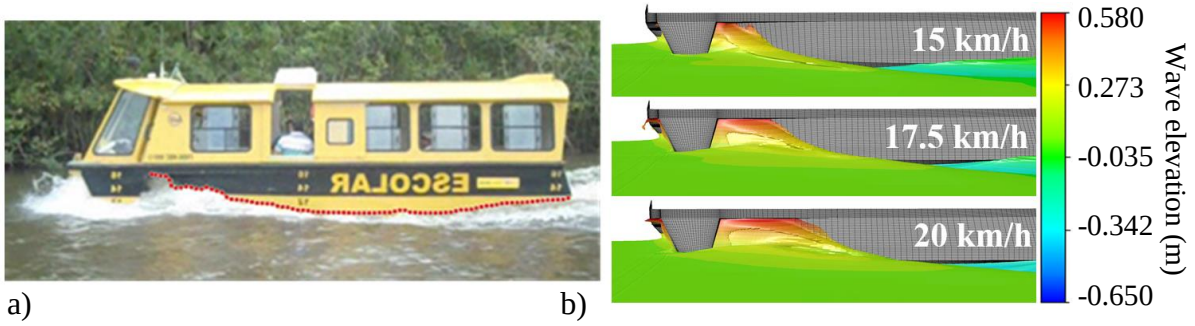


**Figure 5. Wave elevation for the real school boat (a) and the numerical model (b)**

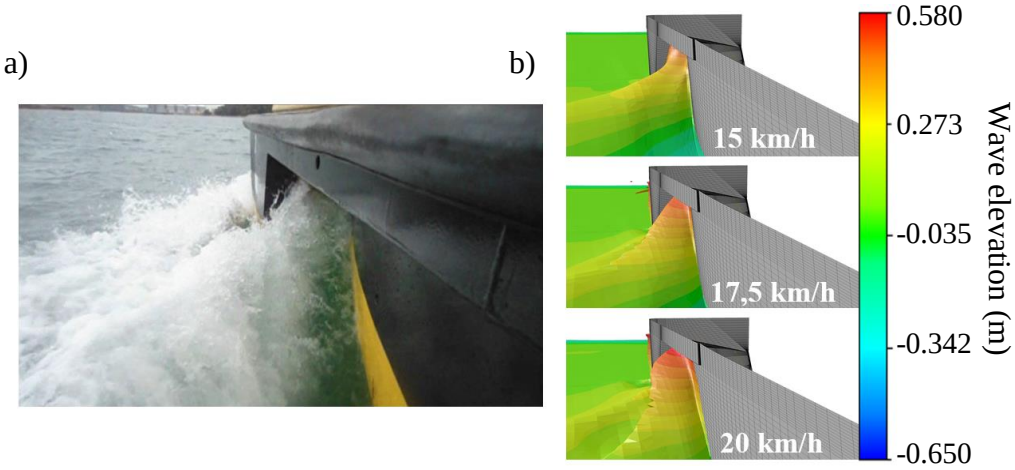


**Figure 6. Wave elevation for the real school boat (a) and the numerical model (b)**

## 7.2 Wave deflector behavior

Initially, a comparison between the two cases concerning the hull resistance was done due to its direct relationship with fuel consumption. As stated previously, velocities varying from 15 to 25 km/h were simulated, and the total time period analyzed was of 1.5 seconds.

It was verified that the difference of resistance between the cases (with and without wave deflector) grows larger by increasing the inlet velocities. This can be explained by the increase of wetted area due to velocity increases. Figure 7 shows the resistance for both cases and the different velocities considered.

It is possible to visualize the resistance is incredibly higher for time periods close to zero. This happens due to the initial conditions of the problem, where the waterline is equal to the design waterline, and the velocity is constant at all the surface and equal to the inlet velocity.

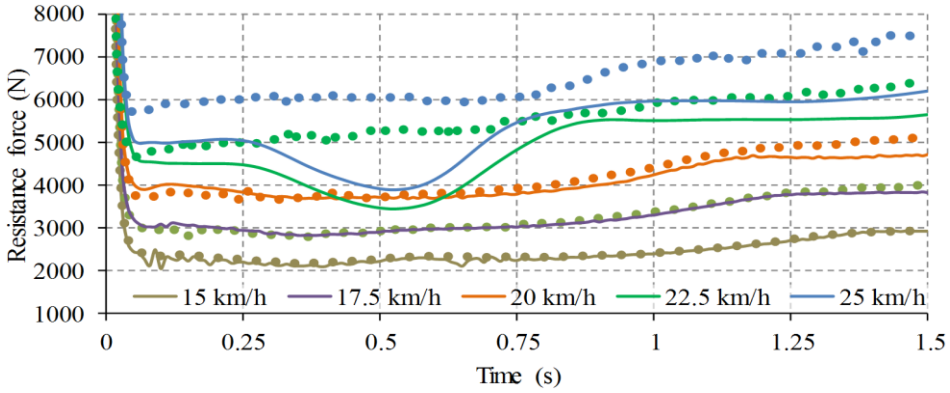


**Figure 7. Resistance force for cases with (dot markers) and without (line curves) the wave deflectors**

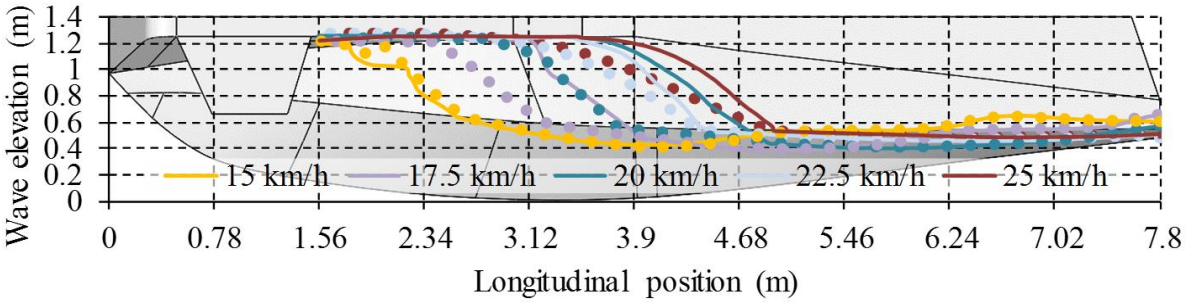


**Figure 8. Wave elevation for cases with (dot markers) and without (line curves) the wave deflector**

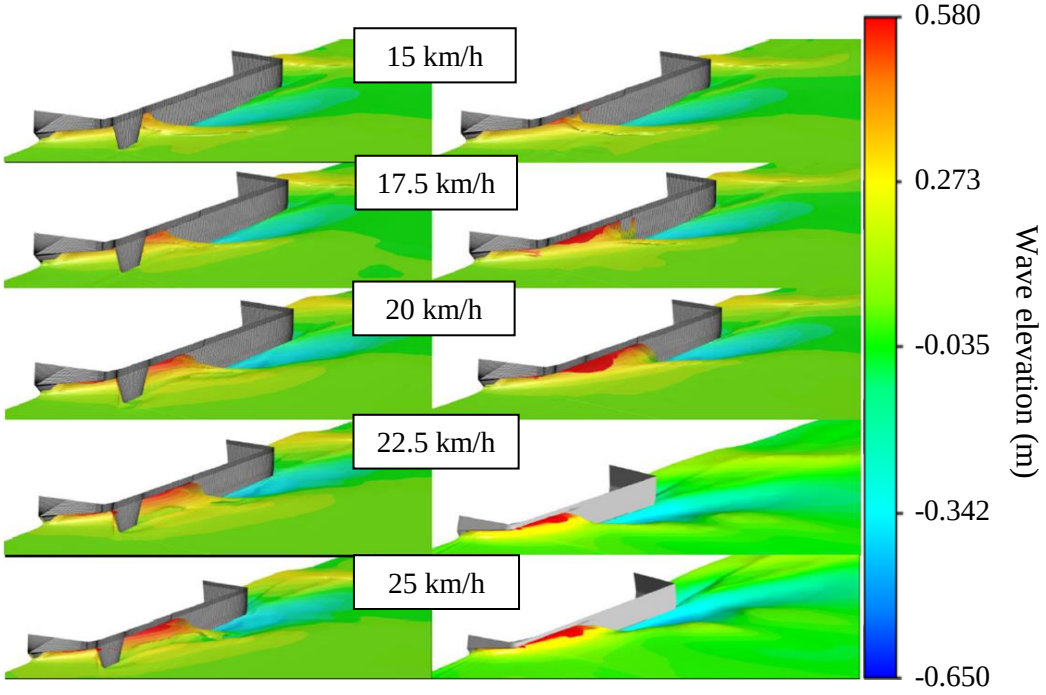


**Figure 9. Free surface views for cases with (left) and without (right) wave deflectors**

The curves of free surface position starting from the end of the wave deflectors were overlapped for the two cases being studied. Figure 8 exhibits those results, where the dot markers represent the cases with wave deflectors, and the line curves represent the cases without it. It is possible to observe that there is not a considerable difference for the wave elevations between the cases for a velocity of 15 km/h. However, the curves start to diverge from the velocity of 17.5 km/h where the wave deflector starts to suppress the elevation of the waves near the hull. This phenomenon is considerable up to 20 km/h; after that the use of wave deflectors has not much effect on wave elevation and generates much more resistance force (as seen in Fig. 7) making those not feasible for higher velocities. This can also be seen in Fig. 9.

# 8 CONCLUSION

School boats are an essential way to facilitate the access of children from riverside communities and poor regions to school environments avoiding school dropout. Nevertheless, this fleet of school boats generates high amplitude wave wake and it can induce erosions and damage fixed or floating structures. To avoid those problems, the evaluation of the hydrodynamic behavior of the school boat was made. In this sense, the CFD software Fluent, was used to obtain results of resistance force and free surface position for two cases, with or without wave deflector surfaces, in order to compare them and evaluate their efficiency.

Since there was no experimental data for the school boat, a Wigley case (Kajitani et al., 1983) was used for validation for being an open multiphasic flow reference concerning hydrodynamic problems. The validation process showed that the mesh is an important part of the model in order to obtain acceptable results. In this sense, hexahedral meshes showed to be harder to be generated for complex geometries; however, they are more accurate to predict the free surface flow in comparison to tetrahedral and prismatic meshes. In addition, the application of numerical diffusion near the non-physical walls through the adoption of a coarse mesh were essential to avoid oscillations of the wave elevation profile at the hull surface. The validation model followed the methodology of Pranzitelli, Nicola, and Miranda (2011), which led to an error below 7% for the resistance coefficient and a similar wave elevation pattern for all Froude numbers analyzed in comparison with the experimental data. Therefore, the model was considered validated.

Two different geometries for the school boat were studied, one with a wave deflector surfaces, and another without it. Both models were created applying the same methodology that was used in the validation case to assure reliable results. There were no experimental results for this case; therefore, the numerical results were analyzed in a qualitative fashion by comparing them to images of the real boat under operation. This analysis suggested that the numerical results were consistent, even though experimental data was still needed to assure the validation of the numerical model for the operation conditions.

Finally, a comparison of the results for the two different cases, with and without wave deflectors, was carried out. It was observed that the two cases have similar performance for a velocity of 15 km/h. The real contribution of the wave deflectors was for velocities of 17.5 and 20 km/h where the wave deflector starts to suppress the elevation of the waves near the hull. Above 20 km/h the use of wave deflectors has not much effect on wave elevation and generates much more resistance force making those not feasible for higher velocities. Nevertheless, the wave deflector represents a good way to reduce the problem of wave

propagation; therefore, its geometry can be optimized for reaching a good efficiency for a wide range of velocities.

## ACKNOWLEDGEMENTS

The research for this paper was financially supported by FNDE with scholarships, without which the present study could not have been completed. A helpful input was received from the colleagues of UFPA who provided insight and expertise that greatly assisted the research. Also, we thank Alessandro Pranzitelli who provided the mesh files for the Wigley case to use as reference.

## REFERENCES

Ahmed, Y., 2011. Numerical simulation for the free surface flow around a complex ship hull form at different Froude numbers. *Alexandria Engineering Journal.* Vol. 50, pp. 229-235.

ANSYS Inc., 2006. ANSYS Fluent Theory Guide Release 11.0. Canonsburg, PA.

Banks, J., Phillips, A. B., Turnock, S, 2010. Free surface CFD prediction of components of ship resistance for KCS. *13th Numerical Towing Tank Symposium.* Duisburg, DE.

FNDE, 2010. Entregues as primeiras lanchas escolares em Belém. <http://www.fnde.gov.br/fnde/sala-de-imprensa/noticias/item/1805-entregues-as-primeiras-lanchas-escolares-em-bel%C3%A9m>. Access on july 24, 2016.

Gao, Z., Yang, H.; Xie, M., 2015. Computation of flow around wigley hull in shallow water with muddy seabed. *Journal of Coastal Research.* Special Issue 73 - Recent Developments of Port and Ocean Engineering, pp. 490 – 495.

Hirt, C. W., Nichols, B. D., 1981. Volume of Fluid (VOF) method for the dynamics of free boundaries. *Journal of Computational Physics.* Vol 39, pp 201-225.

Kajitani, H., Miyata, H., Ikehata, M., Tanaka, H., Adachi, H., Namimatsu, M., Ogiwara, S., 1983. Summary of the cooperative experiment on Wigley parabolic model in Japan. *Proceedings of the Workshop on Ship Wave Resistance Computations.*

Kofoed-Hansen, H., Mikkelsen, A. C., 1997. Wake wash from fast ferries in Denmark. *Fourth International Conference on Fast Sea Transportation (FAST '97)*. Sydney, Australia. Vol. 1, pp. 471-478.

Menter, F. R., 1994. Two-Equation Eddy-Viscosity Turbulence Models for Engineering Applications. *AIAA Journal.* Vol. 32 (8). pp. 1598–1605.

Pranzitelli, A., Nicola, C., Miranda, S, 2011. Steady-state calculations of free surface flow around ship hulls and resistance predictions. *9th Symposium on High Speed Marine Vehicles – HSMV*. Naples, Italy.

Raven, H, 2010. Validation of an approach to analyse and understand ship wave making. *Journal of Marine Science and Technology.* Vol. 15, pp. 331-344.

Souza, A.; Aguiar, C., 2010. Ondas, barcos e o Google Earth. *XII Encontro de Pesquisa em Ensino de Física*. Águas de Lindóia.

Stumbo, S., 1999. The prediction, measurement and analysis of wake wash from marine vessels. *Marine Technology.* Vol. 36, pp. 248-260.

White, F. M, 2010. Fluid mechanics. McGraw-Hill, 5th ed., pp. 467.